Velocity dependence of ionization and fragmentation of methane caused by fast-proton impact

I. Ben-Itzhak, K. D. Carnes, D. T. Johnson, P. J. Norris, and O. L. Weaver
James R. Macdonald Laboratory, Department of Physics, Kansas State Univeristy, Manhattan, Kansas 66506
(Received 26 July 1993)

The velocity dependence of methane ionization and fragmentation have been studied using a coincidence time-of-flight technique. The relative yields of single-ion, ion-pair, and ion-triple channels have been determined for 1- to 12-MeV proton impact. The multiple-ionization cross sections have been determined and are in accord with our model semiclassical Coulomb approximation calculations. The single-ion channels resulting from the breakup of CH_4^{+*} were found to be independent of the collision velocity. Good agreement with previous proton-impact measurements and with electron-impact measurements is observed. On the other hand, the ion-pair breakup channels of CH_4^{2+*} show a surprising dependence on the collision velocity. The ion-pair data are in reasonable agreement with fast-electron-impact measurements at 10 keV while differing significantly with a lower, 1-keV, electron-impact measurement.

PACS number(s): 34.50.Gb, 34.90.+q

I. INTRODUCTION

The fragmentation process of small polyatomic molecules has been investigated for photoionization [1–3], electron impact [4–11], fast-proton impact [11,12], and highly-charged-ion impact [13–15] using various methods. In most of these processes, one electron of the target molecule is ionized resulting in some dissociating states. A small fraction of the target molecules will be doubly ionized and dissociate into ion pairs. Using coincidence between the two charged fragments makes it possible to distinguish this small breakup channel from the main single-ionization channel [2,3,9,10]. The standard picture of these collisions and fragmentation processes is that the electrons will be removed from the molecule rapidly in comparison with the nuclear motion but slowly in comparison with the collision time. Thus, first a transient molecular ion is formed which then either deexcites or dissociates. The momenta of the dissociating fragments comes from the internal excitation of the transient molecular ion. Direct momentum transfer from the projectile is negligible for these fast collisions. With this simple qualitative picture of the fragmentation process caused by fast charged projectiles, one might expect that the branching ratios of the different breakup pathways of each molecular ion will be independent of the collision velocity because the fragmentation occurs once the projectile is far removed from the collision region.

The fragmentation pattern of singly charged methane, the molecule of interest in this work, has been the subject of numerous studies. Some of these focused on a high-resolution measurement of the kinetic-energy distributions of the charged fragments [4–7]. Others focused on the fragmentation pattern (measuring either relative or absolute cross sections) [8–11]. The difference between the fragmentation pattern produced by electron impact or proton impact at the same collision velocity has been discussed by Wexler [11] and by Malhi *et al.* [12], who found in general good agreement between the two. The fragmentation pattern of CH_4^{+*} was found to be independent of the collision velocity as expected at high velocities. Even though the ionization cross sections are small they are still the dominant electron removal process because electron capture is negligible. At the high velocities studied the probability for electron ionization is very small and perturbation-theory calculations are very successful in describing ionization of atomic targets. We will demonstrate that these methods can be applied for molecular targets.

The fragmentation pattern of doubly charged methane has not been studied as extensively. This is due to the complexity of the coincidence experiments and even more because the double-ionization cross sections are approximately two orders of magnitude smaller than the single-ionization cross sections. In spite of these difficulties some early studies were done by McCulloh, Sharp, and Rosenstock [9]. In their work the ion pairs produced by 1-keV electron impact were measured in coincidence and their abundances relative to the $H^+ + CH_3^+$ breakup channel evaluated. Similar measurements for 10-keV electron impact have been done by Backx and Van der Weil [10] which show a somewhat similar fragmentation pattern. The difference between the two measurements, namely, that the 10-keV measurement has a higher rate of breakup channels in which more hydrogen fragments were produced, has been attributed to K-shell ionization which is possible for that electron energy.

In a previous work we investigated the fragmentation pattern of methane caused by 4-MeV proton impact [16]. The different possible pathways leading to each ion-pair channel were discussed and compared to theoretical predictions of Siegbahn [17]. These published data have been included in our systematic study of the velocity dependence of methane ionization and fragmentation caused by fast-proton impact ($v = 6$–22 a.u.) reported in the present paper. The coincidence time-of-flight (CTOF) technique and the experimental apparatus used for these studies have been described in detail elsewhere [18]. The

experimental method is discussed briefly in Sec. II. Our work has focused on the determination of the cross sections for single and double ionization of CH_4. These cross sections are compared in Sec. III A with model calculation using the semiclassical Coulomb approximation (SCA). We have also studied the branching ratios of CH_4^{+*} and CH_4^{2+*} breakup as a function of the collision velocity. The fragmentation pattern of CH_4^{+*} is independent of the collision velocity in agreement with previous proton impact work by Malhi *et al.* [12] and electron-impact studies by Adamczyk *et al.* [8]. In contrast, the fragmentation pattern of CH_4^{2+*} shows an unexpected velocity dependence. This velocity dependence is discussed in Sec. III B.

II. EXPERIMENTAL METHOD AND DATA ANALYSIS

A detailed description of our experimental setup can be found in a previous publication [18]. Briefly, a bunched beam of protons was accelerated in the J. R. Macdonald Tandem Van de Graaff accelerator to the desired energy (1–12 MeV) and then selected by a 90° analyzing magnet. The collimated beam was then directed into a target cell containing methane gas. Pressure in the cell was kept below 0.1 mTorr to ensure single-collision conditions. Ions produced in the cell's collision region were extracted and accelerated by uniform electric fields and allowed to drift into a large chevron microchannel-plate detector. The times-of-flight of all ions hitting the detector were then recorded relative to a fast timing signal synchronized to the beam bunch.

The ionization cross section for the $H^+ + CH_4$ collisions is small (of the order of 10^{-17} cm^2) [12], and the double-ionization cross section is expected to be much smaller. Thus the rate of ion pairs produced from the dissociation of CH_4^{2+*} is much smaller than the rate of single ions coming from the dissociation of CH_4^{+*}. It is still possible to measure the ion-pair channels, however, by requiring the coincidence condition fulfilled by both ions hitting the detector in the same event. From the number of counts under the peaks in the single-ion and ion-pair spectra (Figs. 2 and 3 of Ref. [16]) the cross sections for all final products were evaluated as described in detail elsewhere [16,19]. (The data were corrected for the different detection efficiencies of the different breakup channels, random coincidences, lost fragments, ^{13}C isotope, and contaminant ions in the target gas.) The abundances evaluated from the true number of events are given in Table I for the single-ion channels relative to the yield of CH_4^+ final product (that is CH_4^+ resulting from the deexcitation of CH_4^{+*}) and in Table II for the ion-pair channels relative to $H_2^+ + CH_2^+$. Some ion-triple channels relative to $H_2^+ + CH_2^+$ are also given in Table II. The uncommon choice of ion-pair channel for normalization is made in order to reduce errors, the more common $H^+ + CH_3^+$ normalization channel having a relatively large uncertainty due to the high rate of random coincidences. The abundances of all recoil ions independent of their channel of dissociation (mass spectra) are given in Table III.

TABLE I. The abundances of single-ion dissociation channels produced in $H^+ + CH_4$ collisions at 1–12 MeV relative to the CH_4^+ yield (in %). The 4-MeV data presented hereafter were published previously [16].

Channel \ E_p (MeV)	1.0	1.836	2.38	3.0	4.0	6.0	8.0	10.0	12.0
CH_3^+	83.3±0.8	83.7±0.8	83.8±0.8	83.7±0.8	84.1±0.8	83.7±0.8	83.8±0.8	83.7±0.8	84.0±0.8
CH_2^+	13.1±0.2	12.6±0.2	12.2±0.2	12.0±0.3	12.0±0.2	11.8±0.2	11.6±0.2	11.5±0.2	11.5±0.2
CH^+	4.18±0.09	3.90±0.09	3.78±0.09	3.73±0.09	3.69±0.09	3.64±0.08	3.62±0.08	3.54±0.07	3.51±0.07
C^+	0.73±0.05	0.62±0.05	0.59±0.06	0.58±0.05	0.58±0.06	0.61±0.05	0.62±0.04	0.63±0.04	0.60±0.04
H_3^+	0.007±0.001	0.0064±0.0006	0.0055±0.0007	0.003±0.001	0.0048±0.0005	0.007±0.001	0.008±0.003	0.007±0.001	
H_2^+	0.56±0.04	0.50±0.03	0.45±0.03	0.45±0.04	0.44±0.04	0.49±0.03	0.48±0.03	0.47±0.03	0.46±0.03
H^+	8.7±0.4	8.4±0.3	7.6±0.3	7.7±0.4	7.7±0.3	7.6±0.3	7.5±0.3	7.6±0.3	7.4±0.2

TABLE II. The abundances of ion-pair and ion-triplet dissociation channels produced in $H^+ + CH_4$ collisions at 1–12 MeV relative to the $H_2^+CH_2^+$ yield (in %).

Channel \ E_p (MeV)	1.0	1.836	2.38	3.0	4.0	6.0	8.0	10.0	12.0
				Ion pairs					
$H^+ + CH_3^+$	343±24	321±38	289±23	258±10	262±19	252±17	234±16	233.8±9.0	235±20
$H^+ + CH_2^+$	467±13	426±10	417.5±9.4	389±10	390.2±8.1	378±11	366±16	363.2±9.6	370±11
$H^+ + CH^+$	265.0±7.3	274.3±6.0	281.0±6.1	262.3±7.2	274.5±5.5	267.9±8.0	258±11	253.3±6.9	261.4±7.6
$H^+ + CH^+$	265.0±7.3	274.3±6.0	281.0±6.1	263.3±7.2	274.5±5.5	267.9±8.0	258±11	253.3±6.9	261.4±7.6
$H^+ + C^+$	167.8±4.7	182.7±3.8	194.6±4.2	181.4±5.1	190.4±3.8	177.2±5.5	170.3±7.5	172.0±4.8	179.9±5.4
$H^+ + C^{2+}$	5.94±0.46	6.60±0.36	7.75±0.55	7.71±0.53	6.69±0.24	7.00±0.57	5.56±0.94	5.72±0.46	6.51±0.61
$H^+ + H_2^+$	3.72±0.60	4.86±0.36	5.39±0.88	4.02±0.64	4.54±0.40	4.19±0.93	3.49±0.67	4.29±0.65	3.78±0.91
$H_2^+ + CH^+$	8.43±0.56	8.34±0.33	7.59±0.37	7.22±0.57	7.87±0.28	7.48±0.63	7.14±0.86	7.98±0.59	7.42±0.64
$H_2^+ + C^+$	4.32±0.41	4.23±0.20	4.47±0.23	5.24±0.45	4.82±0.18	4.30±0.49	4.25±0.78	4.25±0.41	4.46±0.44
$H_3^+ + CH^+$	1.12±0.18	0.81±0.08	1.00±0.10	1.11±0.18	0.88±0.07	0.80±0.20	0.89±0.19	0.96±0.17	0.90±0.19
				Ion triples					
$H^+ + H_2^+ + C^+$	0.39±0.32	0.64±0.25	0.52±0.24	0.81±0.48	0.69±0.26	1.40±0.77	0.77±0.53	1.38±0.67	0.51±0.40
$H^+ + H_2^+ + CH^+$	0.79±0.48	1.84±0.59	2.96±0.91	2.06±0.88	2.45±0.72	1.66±0.85	3.4±1.3	2.78±1.1	2.4±1.0

TABLE III. The abundances of all recoil ions produced by 1- to 12-MeV proton impact relative to the CH_4^+ yield (in %).

Channel \ E_p (MeV)	1.0	1.836	2.38	3.0	4.0	6.0	8.0	10.0	12.0
CH_3^+	84.1±0.9	84.5±0.9	84.4±0.9	84.3±0.9	84.7±0.9	84.2±0.8	84.3±0.8	84.2±0.8	84.4±0.8
CH_2^+	14.3±0.2	13.8±0.2	13.4±0.3	13.2±0.3	13.1±0.3	12.7±0.2	12.6±0.2	12.4±0.2	12.4±0.2
CH^+	4.8±0.1	4.6±0.1	4.4±0.1	4.4±0.1	4.3±0.1	4.2±0.1	4.2±0.1	4.1±0.1	4.0±0.1
C^+	1.10±0.007	1.05±0.08	1.04±0.08	1.02±0.08	1.02±0.08	0.97±0.07	0.97±0.06	0.98±0.06	0.95±0.06
C^{2+}	0.015±0.003	0.015±0.003	0.015±0.004	0.015±0.004	0.014±0.003	0.015±0.003	0.015±0.003	0.016±0.003	0.016±0.003
H_3^+	0.011±0.001	0.0097±0.0007	0.0092±0.0009	0.007±0.002	0.0077± 0.0007	0.009±0.001	0.010±0.003	0.009±0.001	0.0015±0.0007
H_2^+	0.81±0.05	0.79±0.05	0.73±0.05	0.73±0.05	0.72±0.05	0.73±0.04	0.72±0.04	0.71±0.04	0.68±0.04
H^+	11.4±0.5	11.4±0.4	10.4±0.4	10.3±0.5	10.3±0.4	9.8±0.4	9.6±0.4	9.6±0.4	9.4±0.3

The total production cross section for any fragmentation channel, given in Tables I–III, can be evaluated using the previously measured total cross section for the CH_4^+ channel produced by fast proton impact [12] as follows. For a single-ion channel

$$\sigma(\text{single-ion}) = \sigma(CH_4^+) R \left[\frac{\text{single-ion}}{CH_4^+} \right] \quad (1a)$$

and for ion pairs

$$\sigma(\text{ion-pair}) = \sigma(CH_4^+) R \left[\frac{\text{ion-pair}}{H_2^+ + CH_2^+} \right] \times R' \left[\frac{H_2^+ + CH_2^+}{CH_4^+} \right], \quad (1b)$$

where $R(\text{single-ion}/CH_4^+)$ and $R(\text{ion-pair}/H_2^+ + CH_2^+)$ are the relative single-ion and ion-pair abundances, respectively, given in Tables I–III. The cross sections for the ion-triple channels can be evaluated similarly to the ion pairs. The ratio of $H_2^+ + CH_2^+$ channel to the CH_4^+ channel, $R'((H_2^+ + CH_2^+)/CH_4^+)$, and the total cross section for CH_4^+ channel production [12] needed for these calculations are given in Table IV.

III. RESULTS AND DISCUSSION

A. Velocity dependence of the ionization of methane

From the measurement of all final charged products produced in the $H^+ + CH_4$ collisions one can evaluate the cross sections for single and double ionization of methane. The triple ionization, on the other hand, cannot be determined accurately enough because for CH_4^{3+} breakup a significant number of $H^+ + H^+ + CH_n^+$ ion triples are produced and cannot be detected as discussed in Sec. II. Some of the singly charged methane deexcites and is detected as CH_4^+. On the other hand, the doubly charged molecular ions dissociate rapidly after the collision, and no CH_4^{2+} survives long enough to be detected. The cross section for single ionization is evaluated by summing all single-ion breakup channels and the CH_4^+ molecular ions. In a similar way the cross section for double ionization is determined from the sum of all ion pairs. Even though our measurement does not distinguish between electron removal by capture or ionization (because the final charge state of the projectile was not determined) we can still assume that ionization is the only important process because electron capture by protons is known to be negligible at these high velocities.

The single- and double-ionization cross sections are plotted as a function of collision velocity in Fig. 1. These cross sections monotonically decrease with increasing velocity, as expected from the decrease in the strength of the perturbation with increasing velocity. For fast protons perturbation-theory calculations have been shown to be a good approximation. One such approximation which is easy to use is the SCA for which Hansteen, Johansen, and Kocbach tabulated the ionization probability for the active electron as a function of the collision impact parameter [20]. We have used the independent electron approximation to describe the ionization of the many-electron methane target. We have assumed that only the eight valence electrons play a role in the process while the carbon K-shell electrons are only spectators. Treating all valence electrons as equivalent electrons the multiple-ionization cross section within the independent electron approximation is given by

TABLE IV. The abundance of $H_2^+ + CH_2^+$ breakup channel relative to the CH_4^+ molecular ion and the total CH_4^+ production cross sections from Ref. [12]. (The asterisk denotes values extrapolated from the data in the reference.)

E_p (MeV)	$R\left[\frac{H_2^+ + CH_2^+}{CH_4^+}\right]$ (%)	$\sigma(CH_4^+)$ (10^{-16} cm^2) Ref. [12]
1.0	0.216±0.030	0.78±0.27
1.836	0.233±0.032	0.56±0.20*
2.38	0.226±0.031	0.48±0.17*
3.0	0.233±0.032	0.41±0.14*
4.0	0.277±0.031	0.38±0.13
6.0	0.197±0.027	0.27±0.09
8.0	0.200±0.028	0.19±0.07
10.0	0.200±0.027	0.12±0.04
12.0	0.190±0.026	0.15±0.05*

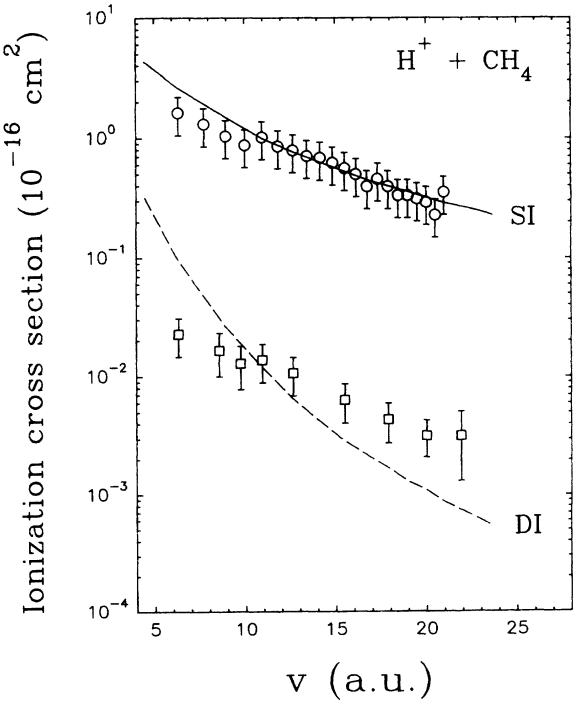

FIG. 1. Single- and double-ionization cross sections of methane by fast-proton impact. The lines are the SCA model calculations.

$$\sigma^{(n)}=2\pi\int_0^\infty db\, b\, P_{\rm ion}^{(n)}(b)$$

$$=2\pi\int_0^\infty db\, b \begin{bmatrix} N \\ n \end{bmatrix} p_{\rm ion}^n(b)[1-p_{\rm ion}(b)]^{N-n}\,, \qquad (2)$$

where n is the number of ionized electrons, $N=8$ is the number of equivalent electrons, and $p_{\rm ion}(b)$ is the ionization probability of the active electron taken from the tables in Ref. [20]. One difficulty in using the active electron probabilities from these tables is the fact that they were calculated for atomic target electrons using hydrogenic wave functions. Clearly the methane molecular target wave functions are more complicated than those hydrogenic wave functions. But it is known that the methane valence electron wave functions are approximately spherically symmetric, thus approximating them with hydrogenic $1S$ wave functions is not unreasonable. The value of the effective charge $Z_{\rm eff}$ seen by the methane valence electron, described by such a hydrogenic S wave function, was determined by fitting the calculated single-ionization cross section to the measured one at 4-MeV projectile energy. The resulting value of $Z_{\rm eff}=1$ was then used for all impact energies. The calculated cross sections, shown in Fig. 1, are in reasonable agreement with the data, especially if one considers the simplicity of our model. The calculated double-ionization cross sections have a stronger velocity dependence than the experimental data. One expects autoionization processes to become more important in comparison with direct ionization as the collision velocity increases, because autoionization does not decrease with increasing velocity while direct ionization does. This autoionization mechanism was not included in our model, and thus it is not surprising that our model underestimates the double ionization at the faster velocities.

In addition to the evaluation of the total single- and double-ionization cross sections these calculations can be used to study the range of contributing impact parameters. The probability functions $P_{\rm ion}^{(n)}(b)$ for single and double ionization multiplied by the impact parameter b are shown in Fig. 2 as a function of b for the lowest and highest impact energy. Double ionization happens mainly up to ~ 5 a.u. while single ionization extends further to more than ~ 14 a.u. These impact-parameter ranges are constant over the velocity range studied. The decrease of the total cross sections with increasing velocity is due to the decrease in the ionization probability of the active electron $p_{\rm ion}(b)$.

B. Velocity dependence of the fragmentation pattern of methane

The abundance of all recoil ions (i.e., singles, ion pairs, and ion triples) relative to the CH_4^+ molecular ion yield are shown in Fig. 3 as a function of collision velocity for proton and electron impact. In most previous measurements the ion pairs were not separated from the single-ion channels, thus in order to compare our measurements with previous measurements we added the single-ion and ion-pair channels. This is in fact a small correction because single ionization is two orders of magnitude larger

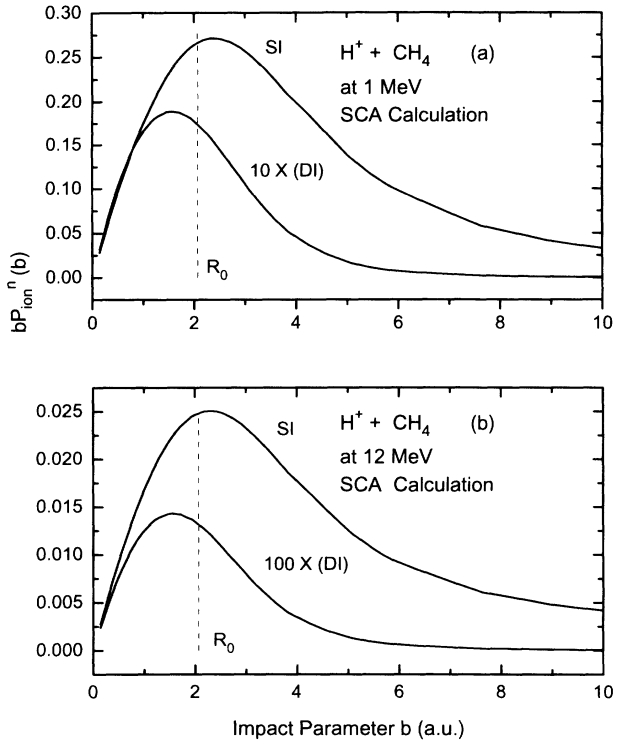

FIG. 2. SCA single- and double-ionization probability functions multiplied by b as a function of impact parameter for (a) 1-MeV and (b) 12-MeV projectile impact energy.

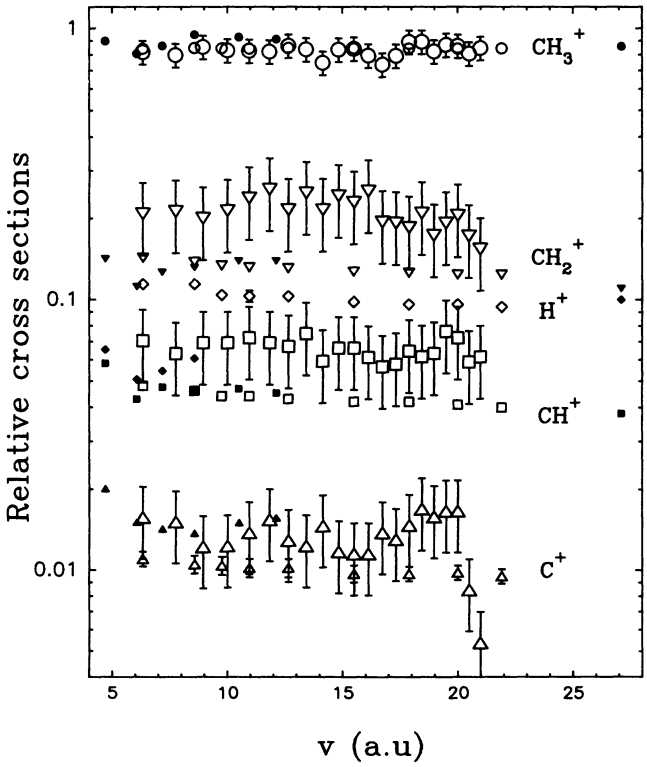

FIG. 3. The velocity dependence of the abundance of the main recoil ions (mass spectra), relative to the yield of CH_4^+, produced by fast proton impact, this work, small open symbols; Ref. [12], large open symbols; and by fast electron impact, full symbols.

than double ionization. The main feature of the fragmentation pattern of CH_4^{+*} is the decrease of the yield of CH_n^+ ions with increasing number of missing hydrogen fragments. These ratios are clearly independent of the collision velocity over the velocity range studied $v=6-22$ a.u. These ratios are in good agreement with previous proton impact data by Malhi *et al.* [12], but the new data have a much higher accuracy. Furthermore, these ratios are in good agreement with electron impact data of Adamczyk *et al.* [8] and Backx and Van der Weil [10], except the H^+ fragment ratios which are approximately a factor of 2 smaller in Adamczyk's data. This might be due to angular discrimination effects which are significant for the light H^+ fragments. The similarities between the electron and proton impact are expected for fast collisions where the first Born approximation is valid because in this approximation the amplitude of the electronic transition is proportional to the projectile charge, and thus the transition probability is proportional to the projectile charge squared (i.e., probabilities scale as q^2/v^2). The process is therefore independent of the sign of the projectile charge.

The abundances of the main ion-pair channels relative to the $H^+ + CH_3^+$ channel are presented in Fig. 4 for electron and proton impact. Our data are in reasonable agreement with the 10-keV electron impact data [10] even though the collision velocity for this electron-impact data is significantly higher. On the other hand, the 1-keV electron-impact data [9] have much smaller relative yields for all channels. The relative abundances for this

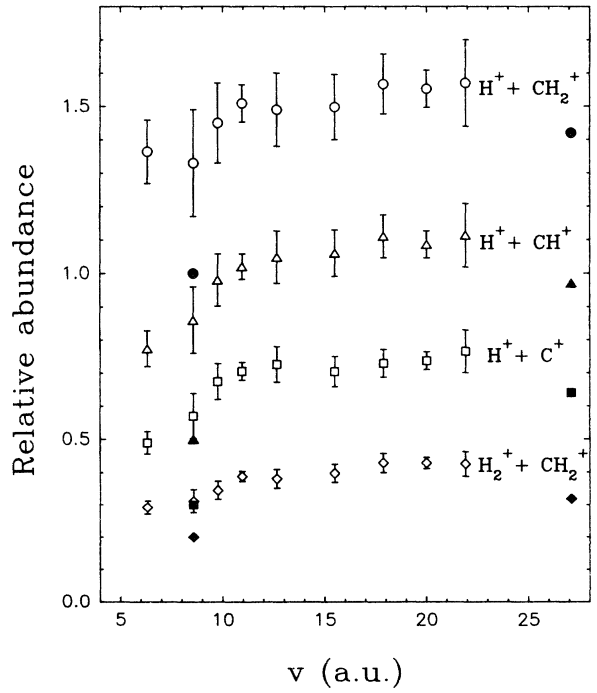

FIG. 4. The velocity dependence of the abundance of the main ion-pair channels, relative to $H^+ + CH_3^+$, produced by fast-proton impact, open symbols; and by fast electron impact, full symbols (the 1-keV data from Ref. [9] and the 10-keV data from Ref. [10]).

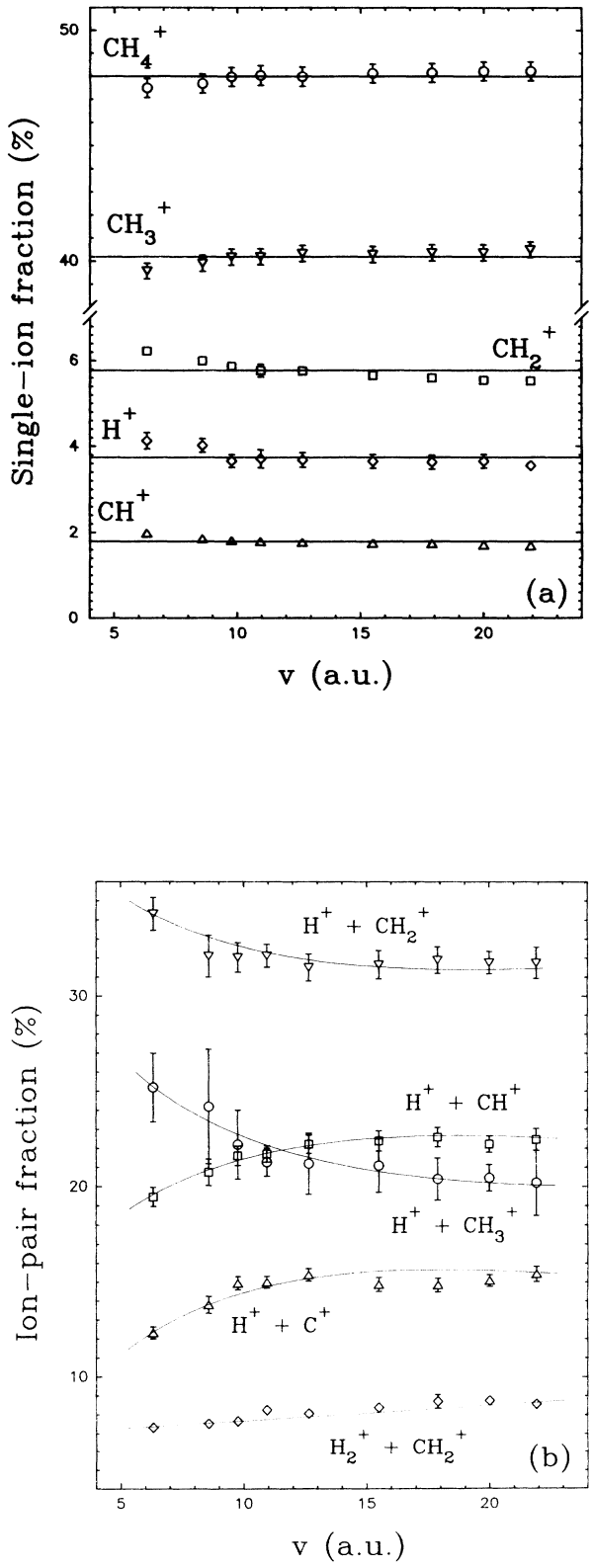

FIG. 5. The fraction of (a) the main single-ion channels out of the total number of single ions, and (b) the main ion pairs out of the total number of ion pairs, as a function of the collision velocity. The lines are drawn to guide the eye.

data set were obtained directly from the number of counts and no corrections were made for efficiency differences or random coincidence rates. We can thus assume that the errors associated with this data set are relatively large. More electron-impact data are needed in order to test the effect of the projectile charge sign on these ratios as has been done for the singly charged methane breakup. For the doubly charged ions one needs to include the second-order term in the Born expansion of the transition amplitude. The second-order term in the Born series, proportional to q^2, is the leading "direct" ionization term. In addition there should be a contribution from ionization of one electron in the first Born approximation, proportional to q, followed by autoionization. When this transition amplitude is squared, a term which depends on the cube of projectile charge q^3 results from "interference" between the first and second Born terms. Thus differences between electron- and proton-impact dissociation of CH_4^{2+*} are possible, and further experiments should be done to investigate this point.

The fraction of the main single-ion channels out of the total number of single ions are plotted in Fig. 5(a) as a function of the collision velocity. The fractions of the main ion-pair channels out of the total number of ion pairs are plotted in Fig. 5(b). In contrast with the lack of velocity dependence of the fragmentation pattern of CH_4^{+*} shown in Fig. 5(a) the fragmentation pattern of CH_4^{2+*} depends on the collision velocity (i.e., the relative importance of the different ion-pair channels is changing with the collision velocity). The abundance of the $H^+ + CH_3^+$ breakup channel, for example, decreases with increasing velocity. On the other hand, the $H^+ + C^+$ breakup channel increases with increasing velocity. This significant difference between the velocity dependence of the fragmentation pattern of CH_4^{+*} and CH_4^{2+*} has no satisfactory explanation as yet. For these fast collisions we do not expect post collision interaction between the projectile and the target fragments to play a role. This is because the collision time ($\sim 10^{-17}$ sec) is much shorter than the dissociation time, which is typically of the order of the vibration time ($\sim 10^{-14}$–10^{-12} sec). Our SCA calculations suggest that the difference in the fragmentation patterns at low and high velocity cannot be attributed to a change in relevant impact parameters. Further studies of the fragmentation pattern of CH_4 are needed in order to help understand this difference in velocity dependence between the singly and doubly charged molecular ions.

IV. SUMMARY

The velocity dependence of ionization and fragmentation of methane have been studied using the CTOF technique. The relative yields of single-ion and ion-pair channels have been determined for 1- to 12-MeV proton impact. The multiple-ionization cross sections have been determined and are in reasonable agreement with our model SCA calculations. In these collisions, mostly singly charged CH_4^+ molecular ions are produced. Most of these molecular ions are unstable and rapidly dissociate into single-ion pairs. The abundances of the single ions resulting from the breakup of CH_4^{+*}, relative to CH_4^+, are similar to the ones measured previously for electron and proton impact, as expected for these fast collisions where the first Born term dominates. The doubly charged CH_4^{2+*} molecular ions dissociate rapidly into ion pairs. The abundances of the main ion-pair channels relative to $H^+ + CH_3^+$ are in good agreement with the 10-keV electron-impact data. On the other hand, 1-keV electron impact tends to be less efficient in producing many hydrogen fragments. The single-ion channels were found to be independent of the collision velocity. In contrast, the ion-pair breakup channels of CH_4^{2+*} show a surprising velocity dependence.

ACKNOWLEDGMENTS

We wish to thank Professor T. J. Gray and Dr. V. Krishnamurthi for many useful discussions. This work was supported by the Division of Chemical Sciences, Office of Basic Energy Sciences, Office of Energy Research, U.S. Department of Energy. D. T. J. and P. J. N. were partly supported by the National Science Foundation.

[1] B. Brehm and E. V. Puttkamer, Z. Naturforsch. A **22**, 8 (1967).
[2] J. H. D. Eland, Mol. Phys. **61**, 725 (1987), and references therein.
[3] G. Dujardin, D. Winkoun, and S. Leach, Phys. Rev. A **31**, 3027 (1985), and references therein.
[4] J. Appell and C. Kubach, Chem. Phys. Lett. **11**, 486 (1971).
[5] Von R. Fuchs and R. Taubert, Z. Naturforsch. A **19**, 494 (1964).
[6] H. Chatham, D. Hils, R. Robertson, and A. Gallagher, J. Chem. Phys. **81**, 1770 (1984).
[7] O. J. Orient and S. K. Srivastava, J. Phys. B **20**, 3923 (1987).
[8] B. Adamczyk, A. J. H. Boerboom, B. L. Schram, and J. Kistemaker, J. Chem. Phys. **44**, 4640 (1966).
[9] K. E. McCulloh, T. E. Sharp, and H. M. Rosenstock, J. Chem. Phys. **42**, 3501 (1965).
[10] C. Backx and M. J. Van der Weil, J. Phys. B **8**, 3020 (1975).
[11] S. Wexler, J. Chem. Phys. **41**, 2781 (1964).
[12] N. B. Malhi, I. Ben-Itzhak, T. J. Gray, J. C. Legg, V. Needham, K. Carnes, and J. H. McGuire, J. Chem. Phys. **87**, 6502 (1987).
[13] R. J. Maurer, C. Can, and R. L. Watson, Nucl. Instrum. Methods B **27**, 512 (1987).
[14] H. Tawara, T. Tonuma, H. Kumagai, and T. Matsuo, Phys. Scr. **42**, 434 (1990), and references therein.

[15] T. J. Gray, J. C. Legg, and V. Needham, Nucl. Instrum. Methods B **10/11**, 253 (1985).
[16] I. Ben-Itzhak, K. D. Carnes, S. G. Ginther, D. T. Johnson, P. J. Norris, and O. L. Weaver, Phys. Rev. A **47**, 3748 (1993).
[17] Per E. M. Siegbahn, Chem. Phys. **66**, 443 (1982).
[18] I. Ben-Itzhak, S. G. Ginther, and K. Carnes, Nucl. Instrum. Methods B **66**, 401 (1992).
[19] I. Ben-Itzhak, S. G. Ginther, and K. D. Carnes, Phys. Rev A **47**, 2827 (1993).
[20] J. M. Hansteen, O. M. Johansen, and L. Kocbach, At. Data Nucl. Data Tables **15**, 305 (1975).